HYDRODYNAMICS PERFORMANCE OF THE TWIN BLADE HYDROFOIL ARRANGEMENT FOR POSSIBLE APPLICATIONS OF WIND AND HYDROKINETIC TURBINES

Yavuz T.* and Koc E.
*Author for correspondence
Department of Mechanical Mechanical Engineering,
Baskent University,
Ankara,
Turkey,
E-mail: tyavuz@baskent.edu.tr

ABSTRACT

Hydrodynamic performance of a twin-blade hydrofoil in the range of the tip speed ratio from 1.5 to 5.5 has been numerically and experimentally investigated. The geometry of the twin blade hydrofoil is presented in the figure below. FLUENT and ANSYS numerical analysis programs were used in the two and three dimensional analysis respectively. At the design flow velocity of 2 m/s (Re = 3.02×10^5) the maximum power coefficient of 0.457 was obtained at the tip velocity ratio of 3.5 at an optimum geometric parameters of h/c_1 = 0.667, c_1/c_2 = 0.67 and the angle of attack of 3°. This tip speed ratio is considered to be low comparing others applications such as hydrofoil-slat arrangements and standard hydrofoil applications. Therefore the double blade arrangements can be used in the wind and hydrokinetic turbines to produce electric energies at moderate low wind and hydrokinetic current velocities.

INTRODUCTION

In several countries many alternative studies for increasing the potential of use of renewable energy systems are recently under way in order to generate new and sustainable solutions for energy crisis and environmental-climatic problems in the world. As known, the main source of the energy is the solar energy. The solar energy of the sun is converted to the other renewable energies such as wind, wave, hydraulic and biogas energies. The sustainable energy has been defined as effectively, the provision of energy such that it meets the needs of the present without compromising the ability of future generations to meet their own needs. The sustainable Energy has two key components: renewable energy and energy efficiency. The wind energy plays very important role in the sustainability of energy. There is another alternative energy resource that is hydro-kinetic power conversion, which is at the same time more stable, continuous, and sustainable. Although this technology may be very little known, water turbines (similar to wind turbines) that can operate in deep channels with stable (constant) flows have been designed, manufactured and operated. Some countries have great hydro-kinetic potential with large and long rivers, water channels with stable and high flow rates, and Turkey is indeed quite fortunate in this respect.

There are three work areas in the wind turbines. These are; the performance analysis of wind turbine blades aimed to increase the rotor efficiency, the design of the concentrator of small scale wind turbines aimed to increase the free wind speed at the inlet of the wind turbine, and to increase the efficiencies of the other components such as gear box, generator and other elements aimed to increase overall performance of the wind turbines system. The blade or rotor which converts kinetic energy of the wind or water current into mechanical energy is the most important component of the turbine systems. Traditionally, wind turbines use the classical standard airfoils which have the maximum lift coefficient of about 1.3 before the stall. Using the different airfoil arrangement such as airfoil with slat and double blade airfoils increase the stall angle of attack and consequently increase the maximum lift coefficient and efficiency of the turbine.

In this study, the double blade was chosen and the optimum geometric dimensions and flow conditions for the high hydrodynamic performance of the system were determined. Results are also applicable for the wind energy and wind turbines.

NOMENCLATURE

α	[°]	Angle of attack, degrees
c_1	[m]	Small blade chord length
c_2	[m]	Large blade chord length
h	[m]	Gap between airfoils
U	[m/s]	Free stream velocity
C_L	[-]	Lift coefficient
C_D	[-]	Drag coefficient
P	[W]	Power
C_p	[-]	Power coefficient
λ	[-]	Tip speed ratio
λ_r	[-]	Local tip speed ratio
B	[-]	Number of blade
φ	[°]	Angle of relative wind or water
ω	[rad/s]	Angular velocity
N	[rpm]	Rotational speed

HYDRODYNAMIC MODEL

Details of the hydrodynamic model are given in Ref. 1 and 2. In the hydrodynamic model, the blade – element momentum theory which is a combination of two different theories, namely the conservation of momentum theory and the blade element theory is used. Conservation of momentum theory refers to a control volume analysis of the forces at the rotor plane based on the conservation of linear and angular momentum. Conservation of momentum states that the loss of pressure or momentum through the rotor plane, which occurs as the fluid passes through the rotor plane, is caused by work done on the turbine blades by the moving fluid. The conservation of momentum theory then allows calculation of the induced velocities in the axial and tangential directions from the momentum lost by the moving fluid. A flow field, characterized by the axial and angular induced velocities, is used to define the local flow conditions at the rotor hydrofoils. Blade-element theory is an analysis of forces which assumes that the blades can be divided into many smaller elements which act independently of surrounding elements. Given the local flow conditions and the blade geometry, the hydrodynamic forces on these blade elements can be calculated. Blade-element theory then sums these elemental forces along the span of the blade to calculate the total forces and moments exerted on the turbine.

High-lift systems essentially modify the fluid dynamics of wings so as to avoid aircraft stalling and methods have been devised to predict boundary layer separation that causes stalling [3, 4]. Stall at high angles of attack can be retarded by either optimizing the shape of the airfoil or by adding high-lift devices such as leading-edge slats and trailing-edge flaps. The optimization of airfoils for high lift is governed by the maximum lift coefficient available from a mono-element airfoil with un-separated flow and the shape of the airfoil can be improved for high-lift situations [5–7]. Leading-edge slats are known to help avoid leading edge separation at low speeds by injection of high-momentum fluid through the gap between the slat and the main airfoil. This injected fluid adds kinetic energy to the boundary layer [8] and hence delays leading-edge separation. Various forms of leading-edge devices have been tested, notably the fixed slat [9, 10, 11], the retractable slat [12, 13], and the Krüger flap [14]. The effectiveness of the leading edge auxiliary airfoil is dependent on its positioning. Same kind of flow behaviour can be observed in the flow around double blade airfoils. In the case of using double-blade airfoil, the fluid dynamics governing the flow field eliminates the separation bubble by the injection of the high momentum fluid through the gab of the double blade of airfoil by meaning of the flow control delays the stall up to an angle of attack.

The main purpose of this study is to present the optimum geometric parameters and flow characteristics for double blade hydrofoil, defined as high performance hydrofoil, useful for hydrokinetic turbine to generate electric energy in rather low hydrokinetic current. Geometric parameters of the double blade hydrofoil are shown in Figure 1. The mean hydrofoil has a 195 mm chord. The variations of the geometric parameters in the analysis were chosen to be as $0.177 < h/c_1 < 0.834$, $0.537 < c_1/c_2 < 0.737$, angle of attack, $0^o < \alpha < 32^o$ and the Reynolds number ($Re = Uc_1/\nu$) $3.02x10^5$.

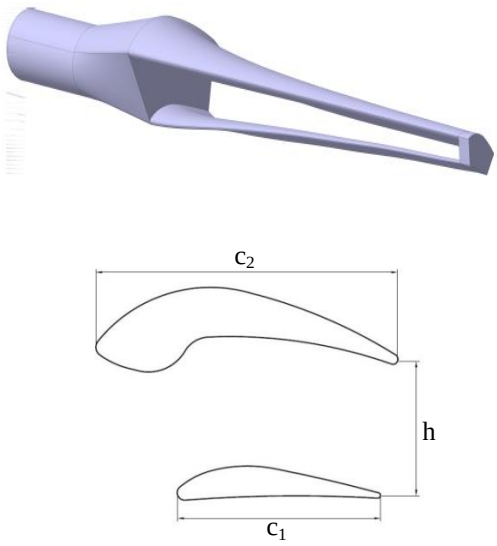

Figure 1 Geometry of double blade hydrofoil

The FLUENT code was used as the advanced tool in this study. Detailed analysis was made using the FLUENT code including Spalart - Allmaras, k-ε turbulent model. The results are all obtained for two dimensional computations although three dimensional effects are present within the separated region. No-slip boundary conditions are used at solid surfaces. The grid used for the double blade hydrofoil is generated by the GAMBIT [15] program, and is shown in Figure 2. The grid extends from 7 chords upstream to 15 chords downstream. The upper and lower boundary extends 12 chords from the profile. Different size grids are used to ensure grid independence of the calculated results. This is achieved by obtaining solutions with increasing number of grid nodes until a stage is reached where the solution exhibits negligible change with further increase in the number of nodes. Consequently, the grid size giving the grid-independent results are selected and the total number of cells is adopted as 42261 nodes.

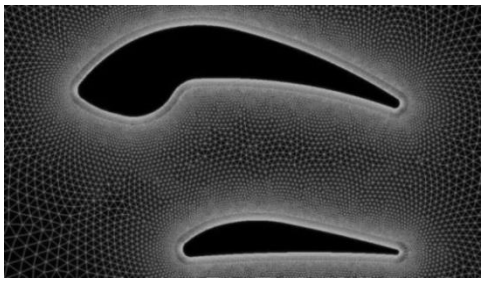

Figure 2 Structured grid of double blade hydrofoil

The FLUENT code solves the RANS equations using finite volume discretization. Second-order upwind discretization in space is used, and the resulting system of equations is then solved using the SIMPLE coupled solution procedure until certain convergence criteria are satisfied. The convergence rate is monitored during the iteration process by means of the residuals of the dependent variables of the governing

differential equations. Convergence is also checked using the relative differences between two successive iterations for each of the integrated force and moment coefficients.

The results shown in this study were obtained for two and three dimensional computations. Free stream boundary conditions were used in the upstream, downstream, and outer boundaries. No-slip boundary conditions were used at solid surfaces. In order to resolve the boundary layer, 10 layers were introduced and first layer is 0.1mm from the wall. Hence the first grid point off the wall in the normal direction was placed at a distance less than $y^+ = 10$ in wall coordinates.

RESULT AND DISCUSSION

The variations of the geometric parameters, as indicated above were chosen to be as $0.177 < h/c_1 < 0.834$, $0.537 < c_1/c_2 < 0.737$, angle of attack, $0^o < \alpha < 32^o$ and the Reynolds numbers ($Re = Uc_1/\nu$), $3.02x10^5$. The design parameters, so called optimum parameters, for wind or hydrokinetic turbines are defined at the maximum value of the ratio of the lift coefficient to the drag coefficient, C_L/C_D with respect to the geometric and flow parameters. Calculations were curried out in the water and the air at two design velocities of 2 m/s and 12 m/s ($Re = 1.025x10^5$) respectively. Results show that, the optimum geometric parameters of the double blade hydrofoil were obtained to be as $c_1/c_2 = 0.671$ and $h/c_1 = 0.667$.

Hydrodynamic performance characteristics of the hydrofoils at the optimum geometric parameters are presented in Table 1 and Table 2 for water and air. As seen in the Tables, the maximum values of the C_L/C_D, 12.053 and 10.75 were obtained at $\alpha = 3^o$ for both cases. There is 10.8 percent difference between two values. This difference can be contributed to the numerical uncertainty. Hence, the design parameters are, for water, $C_L/C_D = 12.05$, $C_L = 1.67$, $C_D = 0.139$ and $\alpha = 3^o$. Maximum lift coefficient, $C_{Lmax} = 2.44$ was obtained at the angle of attack, $\alpha = 30^o$ and then hydrofoil became to the stall condition.

To make a comparison, hydrodynamics performance of the NACA4412 [2], the design parameters of the NACA4412 hydrofoil are $C_L/C_D = 21.52$, $C_L = 0.92$, $C_D = 0.043$ and $\alpha = 6^o$. System becomes to the stall condition about the angle of attack about 14^o. Comparing these two results, the double blade hydrofoil gives lift coefficient of 1.67 which is % 45 higher than that of the value of 0.966 for the single NACA4412 hydrofoil. But, it would pay some penalty of higher drag coefficient.

Table 1 Hydrodynamic performance of the twin blade for water $c_1/c_2 = 0.671$, $h/c_1 = 0.667$ and $Re = 3.02x10^5$

α	C_L	C_D	C_L/C_D
0	1.3698	0.1188	11.5303
2	1.5771	0.131	12.0389
3	1.6706	0.1386	12.0534
4	1.7568	0.1474	11.9186
6	1.899	0.1685	11.27
8	1.9959	0.196	10.1832
10	2.0415	0.2322	8.79199
12	2.0577	0.2773	7.42048
14	2.1068	0.3216	6.551
16	2.1818	0.3646	5.98409
18	2.2518	0.4088	5.50832
20	2.3149	0.4553	5.08434
22	2.3641	0.5039	4.69161
24	2.4038	0.5555	4.32727
26	2.4302	0.6097	3.98589
28	2.4389	0.6659	3.66256
30	2.4413	0.7265	3.36036
32	2.4259	0.7898	3.07154

Table 2 Hydrodynamic performance of the twin blade for air $c_1/c_2 = 0.671$, $h/c_1 = 0.667$ and $Re = 1.025x10^5$

$\alpha(^o)$	C_L	C_D	C_L/C_D
0	1,1775	0,1131	10,4111
2	1,3441	0,1259	10,6759
3	1,447	0,1346	10,7504
4	1,5148	0,1452	10,4325
6	1,5965	0,1751	9,11765
8	1,6218	0,2183	7,42923
10	1,7121	0,2555	6,70098
12	1,8253	0,2914	6,2639
14	1,9374	0,3285	5,89772
16	2,0374	0,3674	5,54545
18	2,1311	0,4094	5,20542
20	2,2048	0,4532	4,86496
22	2,267	0,5	4,534
24	2,3085	0,5497	4,19956
26	2,34	0,6039	3,87481
28	2,3487	0,6623	3,54628
30	2,3376	0,727	3,21541

Pressure distribution, pressure contours and velocity contours over the double blade hydrofoil at optimum geometric and flow conditions are presented in Figure 3. As seen in Figure 3a, pressure reaches a minimum values about -5.0 kPa in the upper chamber and maximum values about 2.3 kPa in the lower chamber regions. Looking the pressure distributions, each blade has very important contributions to the lift forces of the double blade hydrofoils.

Velocity contours around show that maximum velocity, 3.56 m/s (with respect to the mean velocity of 2 m/s) appears to be around leading edge of the large hydrofoils and there are some small flow separation regions in the lower chamber region of large hydrofoil and trailing edges of both hydrofoils.

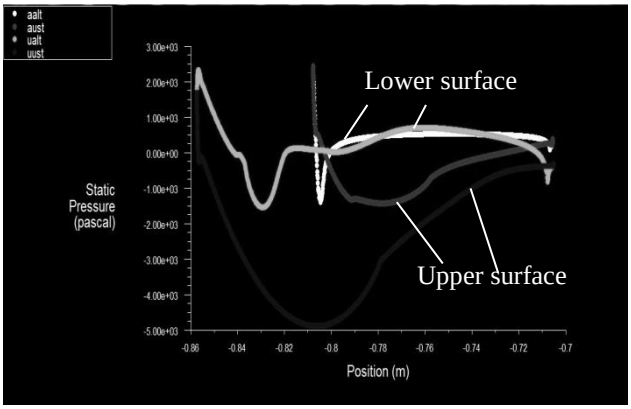

(a)

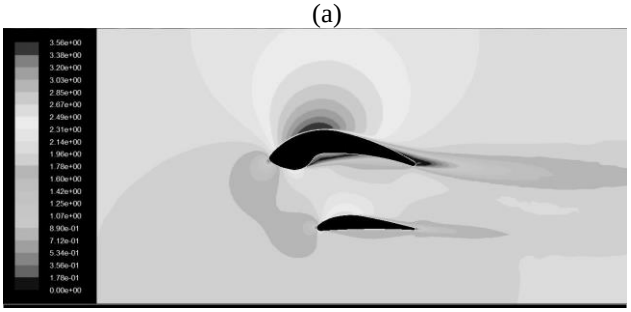

(b)

Figure 3 (a) Pressure distribution (b) Velocity distribution

The power coefficient or efficiency of the double blade hydrofoil can be determined form the formula,

$$C_P = \frac{8}{\lambda^2}\int_{\lambda_k}^{\lambda} \sin^2\varphi(\cos\varphi - \lambda_r \sin\varphi)(\sin\varphi + \lambda_r \cos\varphi)[1-(C_D/C_L)\cot\varphi]\lambda_r^2 d\lambda_r$$

where λ_r is the local tip speed ratio. Performance of the double blade hydrofoil with the optimum geometric parameters is presented in Table 3. As seen from table, the maximum power coefficient, 0.457 is obtained at the tip speed ratio of 3.5. The optimum tip speed ratio of the standard three blade wind turbine is about 5.0. Thus, the optimum tip speed ratio of the double blade hydrofoil, 3.5 is lower than that of the three blade wind turbine, 5.0. Consequently the double blade wind and hydrokinetic turbines can be used at very low wind and current velocities to produce electric energies.

Table 3 Performance of double blade hydrofoil, Re = 3.2 x10^5

Tip speed ratio,λ	**2.5**	**3**	**3.5**	**4**	**4.5**	**5**	**5.5**
Torque (Nm)	224.1	201.33	176.8	149.7	119.43	90.3	60.11
ω (rad/s)	79.55	95.5	111.4	127.3	143.2	159.2	175
Power (W)	1867.5	2013.3	2062.7	1996	1791.5	1505	1102
Power $1/2\rho V^3 A$	4514.8	4514.8	4514.8	451.8	4514.8	4514.8	4514.8
Power coeff., C_P	0.414	0.446	0.457	0.442	0.397	0.333	0.244

Pressure distributions on the blades are presented in Figure 4 at two sample tip speed ratios of 3.5 and 4.0

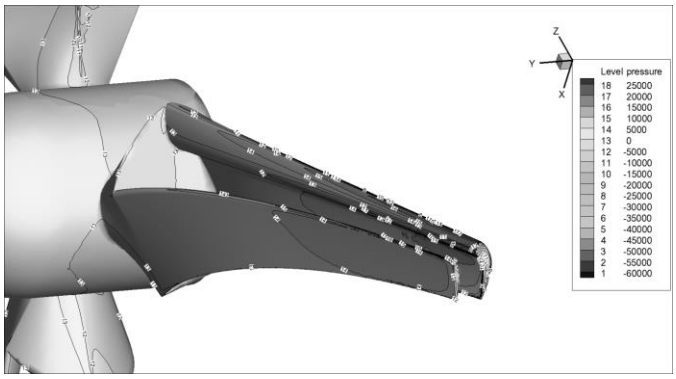

(a) Front surface λ = 3.5

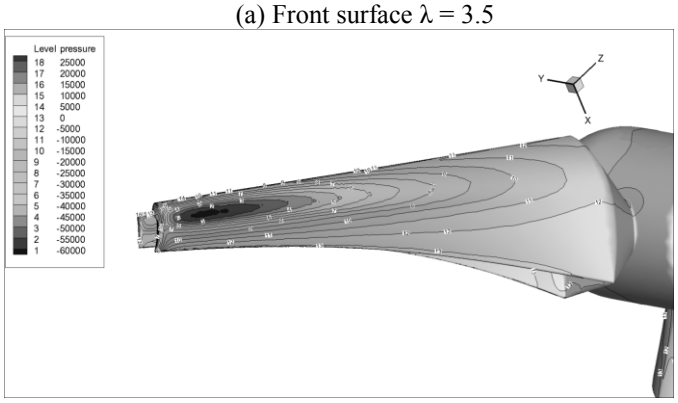

(b) Back surface λ = 3.5

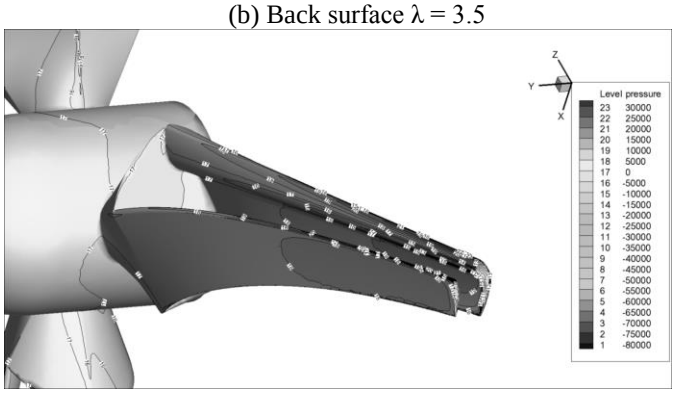

(a) Front surface λ = 4

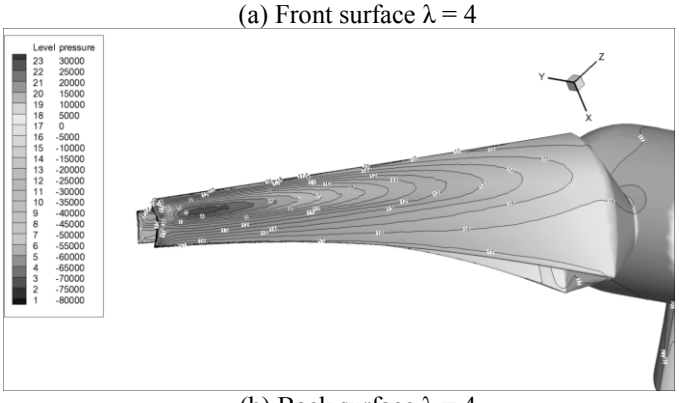

(b) Back surface λ = 4

Figure 4 Pressure distributions on the surface of the double blade hydrofoil.

Hydrokinetic turbines must be designed to avoid cavitations. Pressure on the surface in the operation conditions should not be below to the boiling pressure of the water. Pressure distributions obtained on the front and back surfaces of the blades are presented in Figure 4 at the tip speed ratios of 3.5 and 4.0. The upper side of the airfoils shows the pressure side while the lower side shows the suction side. The rotor considered is lift type and uses lift caused by the pressure difference of the fluid according to the shapes of the cross section of the system. Results show that, as the tip speed ratio increases, the pressure on the front surface of the blade increases while the pressure on the back surface of the blade decreases. The minimum pressure appeared to be in the back region towards to the tip of the blade approximately changes between -60 kPa and -80 kPa from λ = 3.5 to λ = 4. Thus, the surface pressures on the surfaces do not become below the evaporation pressure that may cause the cavitation in the range of the tip speed ratio considered.

The turbulence intensity distributions are also given in Figure 5. The turbulent intensity reaches a maximum in the back regions of the main hydrofoil. The turbulent intensity level in the back region of the main hydrofoil is about 0.25 at λ = 3.5 and it becomes 0.26 at the tip speed ratios of 4.

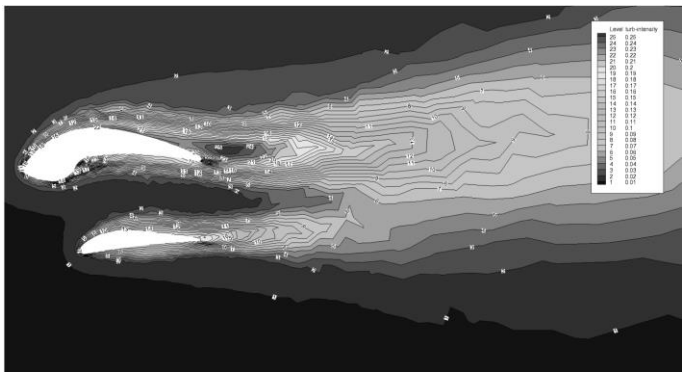

$\lambda = 3.5$

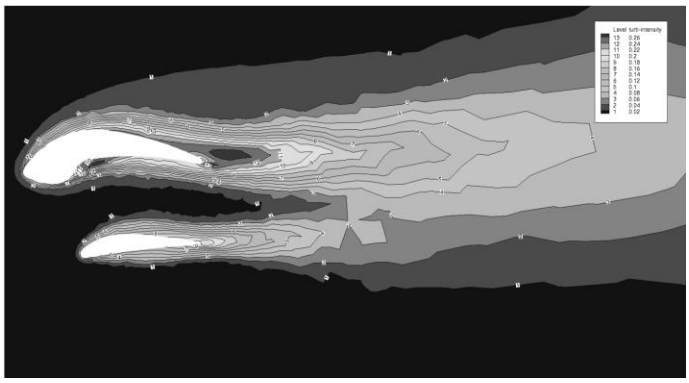

$\lambda = 4$

Figure 5 Turbulence intensity

Also, other study of the double blade hydrofoil application was given in reference [11].

CONCLUSIONS

Flow and performance characteristics of the double blade hydrofoil has been computationally investigated in the range of the Reynolds number $3.02x10^5$ for water. Also some results were given for air Re = $1.025x10^5$. Commercial code FLUENT with Spalart-Allmaras, k-ε turbulent model, was used in the numerical analysis.

Using the double blade hydrofoil, the maximum lift coefficient generated by double blade hydrofoil increases to C_{Lmax} = 2.441 for water and increases to 2.349 for air. The stall angel of attack increases to the value of 30^o and gives the maximum lift coefficient of 2.44. Design parameters are C_L = 1.67 and C_L/C_D = 12.053

The maximum power coefficient of 0.457 obtained at the tip speed ratio of 3.5 which is lower than that of three blades standart airfoils applications.

Using the double blade airfoil or hydrofoil in wind and hydrokinetic turbines, minimum wind velocities and hydrokinetic current velocities to produce economical power will be 3- 4 m /s for wind turbines and 1-1.5 m/s or less for hydrokinetic turbines. Consequently, the wind and hydrokinetic energy potentials of countries will be re-defined and their economic and practical potentials will increase accordingly.

REFERENCES

[1] Yavuz, T., Koc, E., Kılkıs, B., Erol, O., Balas, C., Aydemir, T., Performance analysis of the airfoil-slat arrangements for the hydro and wind turbines applications, *Renewable Energy*, Vol. 74, 414-421, 2015.

[2] Koc, E., Yavuz, T., Kılkıs, B., Erol, O., Balas, C., Aydemir, T., Numerical and experimental analysis of the twin blade hydrofoil for hydro and wind turbine applications, *J.of Ocean Engineering*, Vol. 97, 12-20, 2015.

[3] Stratford, B. S., The prediction of separation of the turbulent boundary layer, *J. Fluid Mech*., Vol. 5, 1–16, 1959.

[4] Cebeci, T., Mosinskis, G. J., and Smith, A. M. O., Calculation of separation points in incompressible turbulent flows, *J. Aircraft*., Vol. 9, 618–624, 1972.

[5] Liebeck, R. H., and Ormsbee, A. I., Optimization of airfoils for maximum lift, *J. Aircraft*., Vol. 7, 409–415, 1970.

[6] Liebeck, R. H., A class of airfoils designed for high lift in incompressible flow, *J. Aircraft*., Vol. 10, 610–617, 1973.

[7] Bingham, G. J., and Chen, A. W., Low-speed aerodynamic characteristics of an airfoil optimized for maximum lift coefficient. *NASA*, No. TN D-7071, Washington, DC, 1972.

[8] Prandtl, L., Motion of fluids with very little viscosity, *NACA TN NO 452*, Washington, DC, 1928.

[9] Weick, F. E., and Sanders, R., Wind tunnel tests of a wing with fixed slots and trailing-edge flap on the lift and drag of a Clark Y airfoil, *NACA Report* No. 472, Washington, DC, 1933.

[10] Genc, S., Kaynak, Ü. and Lock, G. D., Flow over an airfoil without and with a leading-edge slat at a transitional Reynolds number, *Aerospace Engineering*, Vol. 223, 217-231, 2009.

[11] Cengiz, C., Derya, H. T., and Yavuz, T., Investigation of high performance airfoils for wind turbine, *Local Semposium of Wind Energy and Wind turbines*, 11-12 March 2011, Bandırma, Turkey.

[12] Weick, F. E., and Platt, R. C., Wind tunnel tests on a model wing with fowler flap and specially developed leading edge slot, *NACA TN*, No. 459, Washington, DC, 1933.
[13] Schuldenfrei, M. J., Wind-tunnel investigation of an NACA23012 airfoil with a handley page slat and two flap arrangements, *NACA ARR*, No. L-261, Washington, DC, 1942.
[14] Krüger, W., Wind-tunnel investigation on a changed mustang profile with nose flap, force and pressure distribution measurements, *NACA TM* No. 1177, Washington, DC, 1947.
[15] FLUENT (V 6.4) and GAMBIT (V 2.1.6) user's guides, (Fluent Inc., Lebanon, New Hampshire, USA), 2007.